ORIGINAL ARTICLE

Plant, Cell &
Environment PCE WILEY

Plasticity of rosette size in response to nitrogen availability is controlled by an RCC1-family protein

Gustavo Turqueto Duarte[1] | Prashant K. Pandey[1,2] | Neha Vaid[1,3] |
Saleh Alseekh[4,5] | Alisdair R. Fernie[4,5] | Zoran Nikoloski[6,7,8] | Roosa A. E. Laitinen[1,9]

[1]Molecular Mechanisms of Plant Adaptation – group, Max Planck Institute of Molecular Plant Physiology, Potsdam, Germany

[2]National Research Council Canada (NRC-CNRC), Aquatic and Crop Resource Development (ACRD), Saskatoon, Saskatchewan, Canada

[3]Biological Sciences, University of Calgary, Calgary, Alberta, Canada

[4]Central Metabolism — group, Max Planck Institute of Molecular Plant Physiology, Potsdam, Germany

[5]Department of Plant Metabolomics, Center of Plant Systems Biology, Plovdiv, Bulgaria

[6]Systems Biology and Mathematical Modeling – group, Max Planck Institute of Molecular Plant Physiology, Potsdam, Germany

[7]Department of Bioinformatics and Mathematical Modeling, Center of Plant Systems Biology, Plovdiv, Bulgaria

[8]Bioinformatics, Institute of Biochemistry and Biology, University of Potsdam, Potsdam, Germany

[9]Organismal and Evolutionary Research Programme, Faculty of Biological and Environmental Sciences, Viikki Plant Science Centre, University of Helsinki, Helsinki, Finland

Correspondence
Zoran Nikoloski and Roosa A. E. Laitinen, Max Planck Institute of Molecular Plant Physiology, Potsdam, Germany.
Email: nikoloski@mpimp-golm.mpg.de (Z. N.) and laitinen@mpimp-golm.mpg.de (R. A. E. L.)

Funding information
Deutsche Forschungsgemeinschaft, Grant/Award Numbers: LA 3735/1-2, NI 1472/4-2; Horizon 2020 Framework Programme, Grant/Award Number: SGA-CSA No. 739582 under FPA No. 664620; Max-Planck-Gesellschaft

Abstract

Nitrogen (N) is fundamental to plant growth, development and yield. Genes underlying N utilization and assimilation are well-characterized, but mechanisms underpinning plasticity of different phenotypes in response to N remain elusive. Here, using *Arabidopsis thaliana* accessions, we dissected the genetic architecture of plasticity in early and late rosette diameter, flowering time and yield, in response to three levels of N in the soil. Furthermore, we found that the plasticity in levels of primary metabolites were related with the plasticities of the studied traits. Genome-wide association analysis identified three significant associations for phenotypic plasticity, one for early rosette diameter and two for flowering time. We confirmed that the gene *At1g19880*, hereafter named as *PLASTICITY OF ROSETTE TO NITROGEN 1* (*PROTON1*), encoding for a regulator of chromatin condensation 1 (RCC1) family protein, conferred plasticity of rosette diameter in response to N. Treatment of *PROTON1* T-DNA line with salt implied that the reduced plasticity of early rosette diameter was not a general growth response to stress. We further showed that plasticities of growth and flowering-related traits differed between environmental cues, indicating decoupled genetic programs regulating these traits. Our findings provide a prospective to identify genes that stabilize performance under fluctuating environments.

KEYWORDS
Arabidopsis thaliana, GWA, natural variation

1 | INTRODUCTION

Plasticity is the ability of an organism to produce diverse phenotypes in response to changes in the environment. For sessile organisms such as plants, plasticity is particularly advantageous as it allows rapid adjustment to different environments. Nitrogen (N) is an essential component for the production of amino acids, nucleic acids and chlorophyll, and thus directly affects plant growth and development (Guignard et al., 2017; Oldroyd & Leyser, 2020). Plants take up N from the soil primarily as ammonium and nitrate. N distribution in the soil varies both in time and in space resulting in uneven growth among individuals, populations and species (Lark et al., 2004; Pandey et al., 2019). In agriculture, stable crop growth and yield are ensured by applying fertilizers that contain N. However, losses of the large amount of N supplied via fertilization to the environment negatively impact entire ecosystems (Guignard et al., 2017; McAllister et al., 2012). One route towards improved yield, without addition of fertilizers, is to understand the mechanisms underlying plant plasticity responses to N availability. This will allow the development of crop lines with stable growth under varying and unpredictable N availability.

The gene regulatory and metabolic networks for N uptake, assimilation and utilization are well characterized and have been used to improve nitrogen use efficiency (NUE) in plants (Arsova et al., 2012; Fredes et al., 2019; Gutierrez, 2012; Krapp et al., 2011; Li et al., 2017; Meyer et al., 2019; Vidal & Gutierrez, 2008). For instance, modifying the transport of amino acids has been used to improve NUE in pea (Perchlik & Tegeder, 2017). Similarly, DNA methylation and epigenetic mechanisms were found to contribute to the modulation of NUE (Kuhlmann et al., 2020). Given the tight coordination between carbon and N metabolism, genetically improving photosynthesis may also increase NUE and reduce the necessity of fertilizers (Evans & Clarke, 2018). It was also demonstrated that the plasticity in growth-related traits in response to N availability varies between local populations of *Arabidopsis thaliana* (Arabidopsis) (Pandey et al., 2019). Further, Arabidopsis accessions cope with differences in N availability by modifying the root and shoot architecture, growth and biomass (de Jong et al., 2019; Ikram et al., 2012; Masclaux-Daubresse & Chardon, 2011; Meyer et al., 2019; North et al., 2009). In addition, genetic and metabolic changes have been associated with growth under different N availabilities (Scheible et al. 2004; Gaudinier et al., 2018). However, the question of whether or not there are genes that control plasticity of different focal traits to N availability remains open. The answer to this question complement the quest to identify genes underlying the mean value of a given focal trait. The availability of accessions, as genetically homozygous lines (Kramer, 2015; Weigel, 2012), along with a large repertoire of genetic and molecular tools, renders Arabidopsis an excellent model system to address this question.

Despite the high potential of genome-wide association (GWA) in identifying genetic basis of phenotypic variation, only a few studies have used this approach to investigate genotype variation in plasticity among Arabidopsis accessions (Brachi et al., 2013; de Jong et al., 2019; Sasaki et al., 2015). A challenge for mapping genes that control plasticity, hereafter referred to as *plasticity genes*, lies in the quantification of plasticity as a trait. Plasticity can be quantified by different approaches, including, but not limited to linear regression of the reaction norms, the coefficient of variation (CV), plasticity index and fold change (FC) (Laitinen & Nikoloski, 2019; Pennacchi et al., 2020).

Here we focus on dissecting the genetic architecture of plasticity of growth- and flowering- related traits in response to the availability of N in the soil in a panel of Arabidopsis accessions. Growth and development are tightly linked to metabolism, and recent studies have further shown that metabolic variability is genetically controlled (Alseekh et al., 2017; Joseph et al., 2015; Li et al., 2017). Therefore, we also asked if the plasticity of growth- and flowering-related traits could be explained by the plasticity of primary metabolites. Our GWA study revealed that the genetic architecture of the studied plasticities differed. We identified that *At1g19880*, gene encoding for an RCC1 family protein, is involved in controlling the plasticity of rosette size in the beginning of the vegetative growth in response to N. Finally, we investigated if the studied plasticities were specific for different environmental cues, including light and day length. Our results indicated that the mechanisms controlling the plasticity of plant size, flowering time, and yield to N availability are independent from other growth-limiting environmental cues, such as light.

2 | MATERIALS AND METHODS

2.1 | N screening conditions

For phenotyping, 190 *Arabidopsis thaliana* accessions were grown on soil containing limiting, intermediate and optimal amounts of nitrogen and as described in Pandey et al. (2019). The intermediate and optimal N soils were prepared consecutively by aliquoting and increasing the concentration of NH_4NO_3 from the same limiting N soil basis. For each liter of soil, the limiting N soil basis was prepared by mixing 50% (v/v) fine white peat (basic substrate, Gramoflor GmbH, Vechta, Germany), 30% (v/v) fine and 25% (v/v) coarse-grained vermiculite peat (Vertrieb Kausek Gartenbau & Floristikbedarf GmbH, Germany), 2.6 g K_2HPO_4, 3.96 g GRANUKAL 85 (80% $CaCO_3$ & 5% $MgCO_3$-Kreideverke Danmmann KG, Soehlde, Germany) and 10.6 mg Fetrilon-Combi (Spurennährstoffdünger) micronutrient fertilizer (BASF AG, Ludwigshafen, Germany). For the intermediate N condition, 5.44 mg of solid NH_4NO_3 were added per litre of the soil basis, while for the optimal N condition, 54.4 mg of solid NH_4NO_3 were added per litre of soil mixture. To homogenize, the soil mixture was placed at 10°C and mixed every second day for 2 weeks. The accessions were obtained from the Nottingham Arabidopsis stock centre (NASC) and are listed in Table S1. The plants were grown on pots (ø = 6 cm, h = 5.5 cm) containing the same mass of adjusted soil. The seeds were stratified for five days in the dark at 4°C and germinated for one day under short day (8 hr/16 hr) condition at 20°C/16°C and 150 μE m^{-2} s^{-1} of light intensity. To ensure flowering, all accessions were

vernalized for eight weeks at 4°C under long days and light intensity of 7 μE m^{-2} s^{-1}. After this, plants were pricked to new pots (day zero). Four plants in two pots ($n = 4$) were grown under long days at 21°C/17°C (day/night) and 150 μE m^{-2} s^{-1} of light intensity. Early rosette (ERD) diameter was the rosette diameter ten days after pricking and the final rosette diameter (FRD) at the time of flowering. Rosette diameters were manually measured using ImageJ from photos taken from above the pots and at different time points (Schneider et al., 2012). Flowering time (FT) was scored at the day of the first open flower counting since pricking. Seed number yield (YIE) was quantified from two plants together by dividing the total weight of the seeds by the weight of one hundred seeds and multiplying by 100. The N screening data were scored from six experimental batches for ERD, and five for FRD, FT, and YIE. In all experiments, to minimize stochastic variation the replicates were distributed across different trays and the trays were periodically rotated in the growth chamber.

2.2 | Adaptability experiments

For the adaptability experiments, 19 accessions were selected based on their ERD, FT and YIE plasticity to N (Table S8) and germinated on standard Arabidopsis soil. After eight weeks of vernalization, the plants were transferred to long day (16 hr/8 hr), 20°C/16°C (day/night) and light intensity 120 μE m^{-2} s^{-1} for acclimation for one day, following pricking to new pots (day zero). For the experiments under short days, long days (control condition) and low light, five pots with two plants each were prepared for every accession and condition ($n = 10$). For the experiments under high light, five plants were transferred to big pots (ø = 13 cm, h = 10 cm) and in the polytunnel (natural light and temperature), three plants were transferred to big pots (ø = 13 cm, h = 10 cm) in both conditions resulting in $n = 15$. For the experiments under short day (8 hr/16 hr) and the long day control (16 hr/8 hr), the temperature was 20°C/16°C (day/night) and light intensity 120 μE m^{-2} s^{-1}. In the low and high light the plants were grown at long-day 16 hr/8 hr with temperature 21°C/17°C day/night cycle with light intensity of 20 μE m^{-2} s^{-1} (low light) and 750 μE m^{-2} s^{-1} (high light). The experiment in the polytunnel under natural conditions was performed during summer 2020. ERD, FT and YIE were scored as previously described. For the adaptability experiments, seed weight (SW) was inferred from two aliquots of one hundred seeds per plant. SW was measured individually for two plants grown in the polytunnel, and for three plants grown in the other conditions.

2.3 | Metabolite profiling

For the primary metabolites quantification, four plants of the selected set of accessions (Tables S6 and S7) were grown on the same conditions used for the N screening. When the plants reached the ten-leaf stage, they were collected and frozen in liquid nitrogen. Another four plants in two pots were harvested and frozen to liquid nitrogen at mid-day for metabolites analysis at ten-leaf stage. Extraction and

analysis by gas chromatography–mass spectrometry (GC–MS) was performed as described in (Lisec et al., 2006). Briefly, frozen ground material was homogenized in 300 μL of methanol at 70°C for 15 min and 200 μL of chloroform followed by 300 μL of water was added. The polar fraction was dried under vacuum, and the residue was derived for 120 min at 37°C (in 40 μL of 20 mg ml^{-1} methoxyamine hydrochloride (Sigma-Aldrich, cat. no. 593–56-6) in pyridine followed by a 30 min treatment at 37°C with 70 μL of N-methyl-N (trimethylsilyl)trifluoroacetamide (MSTFA reagent; Macherey-Nagel, cat. no. 24589–78-4). The GC–MS system used was a gas chromatograph coupled to a time-of-flight mass spectrometer (Leco Pegasus HT TOF-MS). An auto sampler Gerstel MultiPurpose system injected the samples. Chromatograms and mass spectra were evaluated by using Chroma TOF 4.5 (Leco) and Xcalibur 2.1 software, peak area was normalized by comparison to an internal standard (ribitol; CAS488-81-3) and the fresh weight of the sample used for extraction.

2.4 | Data analysis

For each trait and condition, the mean values were obtained from at least three replicates. Any accession that did not have data for at least three replicates for each condition was removed from the analysis. After filtering the number of accessions used for analysis was 142 for ERD, 109 for FRD, 127 for FT and 102 for YIE. For each accession, the trait values were estimated as the average of the replicates in each condition (Tables S2 and S6). Two plasticity measurements were used namely the fold change (FC) between two conditions and the coefficient of variation (CV) across conditions. The CV was calculated as the standard deviation (σ) divided by the mean (μ) (CV = σ / μ) of the averages of each condition. All statistical analyses were performed in R (https://www.R-project.org/; (Team, 2020)), using RStudio v. 1.3.1056. The correlations were calculated using the *corr.test* function of *psych* package v. 2.0.9 (https://CRAN.R-project.org/package= psych; (Revelle, 2020)), and plotted using the *corrplot* package v. 0.84 (https://github.com/taiyun/corrplot; (Wei, 2017)). The correlations were calculated using Spearman's rank coefficient and pairwise comparisons, and the *p*-values were corrected by the Benjamini–Hochberg procedure. The boxplots were generated using the *ggplot* function of *ggplot2* package v. 3.3.2 (http://www.jstatsoft.org/v40/i01/; (Wickham, 2009)), *ddply* function of *plyr* package v. 1.8.6 (Wickham, 2011), and the *pivot_longer* function of *tidyr* package v. 1.1.2 (https://CRAN.R-project. org/package=tidyr; (Wickham, 2020)). K-means clustering was performed with the *kmeans* function of *stats* package integrated in R (v. 4.0.3), using Hartigan and Wong algorithm. The optimal number of clusters was determined with the Silhouette method using the *fviz_nbclust* function of *factoextra* package v. 1.0.7 (https://CRAN.R-project.org/package=factoextra; (Kassambara, 2020)), using 1,000 bootstrap samples. Heatmaps were plotted using the *ComplexHeatmap* package v. 2.6.2 (Gu et al., 2016). The graphs were further edited using Microsoft Office.

To determine the variance components, we used mixed effect ANOVA, as implemented in anovaVCA function in the R-package

VCA v. 1.4.3 (https://cran.r-project.org/web/packages/VCA/vignettes/VCA_package_vignette.html), with random effects for the genotype and genotype-by-environment interaction and a fixed effect for the environment factor. Variance components were determined based on a model for each batch treated separately, since accessions were randomized within, and not across batches. This experiment design does not have an effect on the estimated nominal measures of plasticity, that is, fold changes and coefficient of variation, since these are calculated for each accession independently of the others.

2.5 | Genome-wide association analysis

GWA analyses were performed using the easyGWAS tool (Grimm et al., 2017) (https://easygwas.ethz.ch/). For each of the complex traits, the averages under limiting, intermediate, or optimal N, the fold change between limiting to optimal N, and the CV across the three N conditions were used as input for GWAS. The analyses were performed with both the 250 K SNPs and the 1,001 whole sequence datasets, using TAIR10 gene annotation. The data were transformed using the BoxCox method, and each analysis was corrected for population structure using the FaSTLMM algorithm. The minimum allele frequency (MAF) cut-off was set to 10%, and only associations with correction significance level $\alpha < 0.1$ using Bonferroni-method were reported (Table 1 and Table S4).

2.6 | Mutant analysis

T-DNA lines for candidate genes were obtained from NASC and are listed in Table S4. Genomic DNA was extracted using the Sucrose Prep method (Berendzen et al., 2005), following genotyping by PCR for the respective T-DNA insertion using the primer pairs listed in Table S9. Homozygous mutant lines were tested on the same conditions used for the N screening experiments at which the genome-wide association was identified, using Col-0 wild type as a reference. In summary, the seeds were stratified and germinated for one day under short day. After eight weeks of vernalization, the plants were acclimated for one day to long days at 21°C/17°C (day/night) and 150 μE m^{-2} s^{-1} of light intensity, before pricking to new pots (day zero; $n = 10$ for each line and condition). Two and three independent experiments were performed to confirm the associations to FT and ERD plasticities, respectively.

To confirm the phenotype of SALK_117261 line (*PROTON1*) in response to optimal and limiting N, mutant plants and Col-0 WT were grown under the conditions described above in three independent experiments. After vernalization of eight weeks and acclimation for one day, the plants were pricked to new pots (day zero, $n = 10$ for each genotype and condition). ERD was scored 10 days after pricking.

To test if *PROTON1*-dependent phenotype was specific to N-promoted responses, vernalized *PROTON1* mutants and Col-0 WT ($n = 10$) were grown on soil that was saturated with 100 mM or 150 mM NaCl on three independent. The soil was saturated with NaCl solutions on the second day after pricking, and then watered with the same solution every second day.

To investigate the ERD plasticity in response to N in a natural mutant of *PROTON1*, Xan-5, Col-0 and Xan-5 plants were grown on limiting and optimal N soils on four experiments as described above ($n = 10$ for each genotype and condition in each experiment) and scored for ERD 10 days after pricking.

2.7 | *PROTON1* promoter sequencing

The promoter region of *At1g19880* was amplified by PCR with *At1g19880*_Prom-Fw and *At1g19880*_Prom-Rv primers (Table S9) for 90 accessions that were part of the initial screen but not in the 1,001 genomes dataset (Table S5). For each accession, a fragment of approximately 1,500 bp was purified from 0.9% agarose gel using NucleoSpin gel and PCR clean-up columns (Macherey-Nagel GmbH & Co KG, catalog 740,609), and Sanger-sequenced using the same primers (LGC, Biosearch Technologies). Sequencing chromatograms were evaluated using Chromas v.2.6.6 (Technelysium Pty Ltd).

TABLE 1 *Significant associations identified for ERD and FT in response to different nitrogen conditions using 250 K SNPs and whole-genome SNPs. GWA analysis was done using easyGWAS web-application (https://easygwas.ethz.ch) with minimum allele frequency of 10% and Bonferroni correction $\alpha = 10\%$*

Trait		Dataset	Chr	Position	Gene ID	Major allele (frequency)	Minor allele (frequency)	*p*-value
ERD	FC	1001	1	6904858	AT1G19880/AT1G19890	C (32)	A (26)	1,75E-07
			1	6904935	AT1G19880/AT1G19890	G (32)	T (26)	1,75E-07
	AVG (Int N)	250K SNPs	1	18698019	AT1G50460	T (120)	C (31)	3,31E-07
FT	FC	250K SNPs	1	27877764	AT1G74140	C (66)	G (66)	5,03E-07
			1	27878486	AT1G74140	G (67)	T (65)	3,11E-07
			1	27878667	AT1G74140	T (71)	C (61)	6,29E-08
			1	27879038	AT1G74140	C (62)	T (60)	7,64E-08
	CV		1	27879038	AT1G74140	C (69)	T (52)	3,34E-07

2.8 | Gene expression analysis

For each line, five pools each containing two rosette of plants grown under optimal or limiting N were harvested to liquid nitrogen 10 days after pricking. Total RNA was extracted using TRIzol reagent (Invitrogen, catalog 15,596,026) and DNA was removed using TURBO DNA-free kit (Invitrogen, catalog AM1907). cDNA was synthesized with the ImProm-II Reverse Transcription System (Promega, catalog A3800). Quantitative real-time PCR reactions were performed using Power SYBR Green PCR-Master-Mix (Applied Biosystems, catalog 4,367,659) and the ABI PRISM 7900HT (Applied Biosystems) system. *EF1ALPHA* (At5g60390), *PP2AA3* (At1g13320) and *SAND* (At2g28390) were used as housekeeping genes (Table S9). For each sample, the target gene levels were normalized by the delta-Ct to the average of the three housekeeping genes. The complete list of primers used for gene expression quantification is provided in Table S9.

3 | RESULTS

3.1 | Plasticity screening using *Arabidopsis thaliana* accessions in response to N availability

We screened 190 Arabidopsis accessions (Table S1), grown on soil supplemented with three different concentrations of N (Methods), for plasticity of focal traits including early rosette diameter (ERD), final rosette diameter (FRD), flowering time (FT) and yield (YIE) (Table S2). A pilot experiment with a subset of accessions, following an established protocol (Pandey et al., 2019), was used to determine the N conditions considered as limiting, intermediate and optimal for growth (Methods). Accessions with missing data in at least one N condition were removed from further analysis, resulting in 142 (ERD), 109 (FRD), 127 (FT) and 102 (YIE) accessions to characterize the plasticity of the four phenotypes. On average, the accessions were larger, flowered earlier and produced more seeds when grown under optimal N in comparison to intermediate and limiting N (Figure 1(a)).

Clustering of the accessions according to their reactions norms, representing the phenotype mean as a function of different environments, partitioned the accessions into three groups for ERD and two groups for each of the other complex traits (FRD, FT and YIE) (k-means clustering, k determined by silhouette index analysis, Figure 1 (b), Table S2). The differences in response of the studied focal traits between the clusters of accessions indicated that there is a genetic variation in plasticity of these traits to N availability.

To quantify plasticity of the focal traits, we calculated the coefficient of variation (CV) of the traits for each accession using the mean values in the three N conditions (Methods, Table S3). The average CVs for all traits were smaller than 1, implying a generally low degree of plasticity (Figure 2(a)). ERD showed higher median plasticity (0.46) than the other traits (Figure 2(a)). In contrast, FT, measured as the number of days from pricking of the seedlings to the first open flower, had the lowest median CV (0.11) in response to the three N conditions (Figure 2(a)). We also asked if the accessions differed with
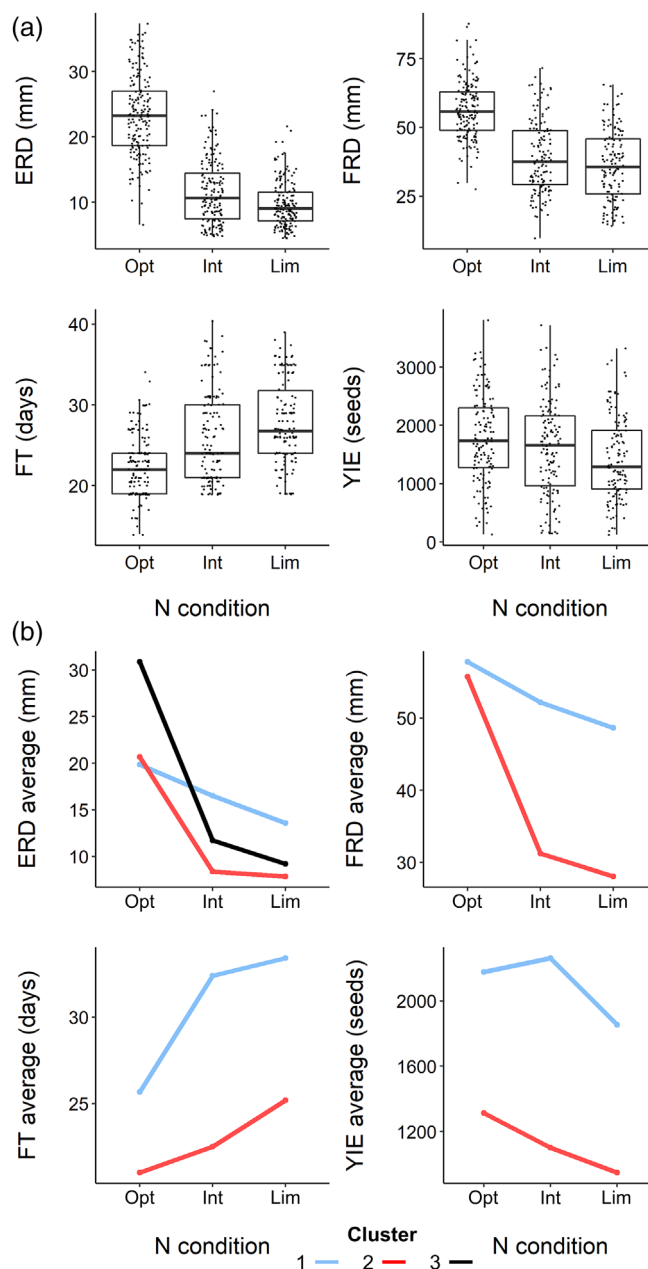

FIGURE 1 *Mean trait values in response to different N availability in Arabidopsis accessions.* Screening of Arabidopsis accessions for early rosette diameter (ERD, n = 176 accessions), final rosette diameter (FRD, n = 155 accessions), flowering time (FT, n = 163 accessions) and yield (YIE, n = 134 accessions) at optimal (Opt), intermediate (Int) and limiting (Lim) N conditions. (a) Boxplots showing the mean values for the complex traits across accessions in each N condition. The line indicates the median value. (b) k-means clustering of the reaction norms representing groups of accessions with similar profiles in response to N availability for early rosette diameter (ERD, n = 142 accessions), final rosette diameter (FRD, n = 109 accessions), flowering time (FT, n = 127 accessions) and yield (YIE, n = 102 accessions) at optimal, intermediate or limiting N. For each cluster, the profile is represented by a different colour. The accessions belonging to each cluster are given in Table S2. The optimal number, k, of clusters for each trait was determined by silhouette index (see Methods). In each trait, the mean trait value is the mean of at least three plants
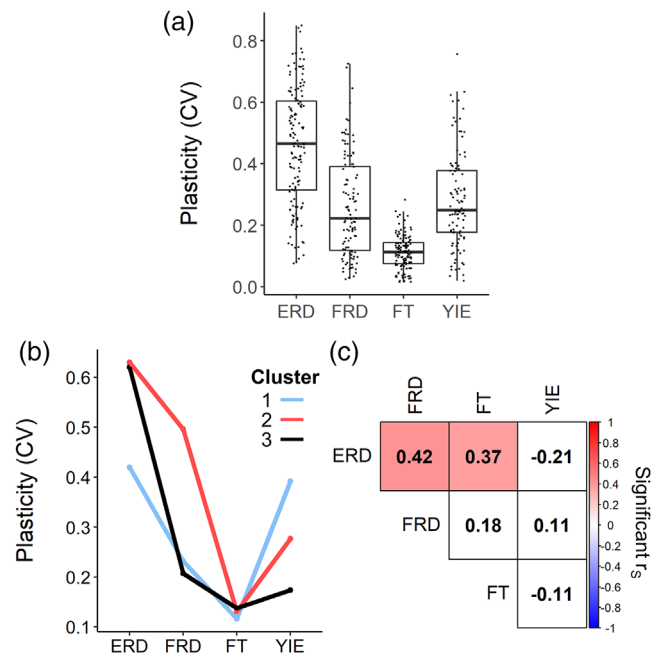
FIGURE 2 *Plasticity of complex traits in response to N availability in Arabidopsis accessions.* (a) Boxplots showing the coefficient of variation (cv) of the accessions for each trait across the three nitrogen conditions (early rosette diameter (ERD), *n* = 142 accessions, final rosette diameter (FRD), *n* = 109 accessions, flowering time (FT), *n* = 127 accessions, yield (YIE) *n* = 102 accessions). (b) Clustering of the accessions based on the coefficient of variations (CVs) for the four phenotypes (*n* = 77 accessions, with the CVs for all phenotypes available). The optimal number of clusters (k) for each trait was determined by silhouette index. (c) Spearman correlation between the coefficient of variation (CV) of complex traits across the three nitrogen conditions. Adjusted *p*-values were calculated using Benjamini-Hochberg correction. Significant r_s correlations (FDR < 0.05) are represented as red, for positive, and blue, for negative [Colour figure can be viewed at wileyonlinelibrary.com]

respect to the pattern of plasticities for the four focal traits. To this end, we clustered the 77 accessions for which the CV of all four focal traits were measured, and found that they can be partitioned into three groups (Figure 2(b); Table S3). The accessions in cluster 1 showed lower plasticity in the ERD than those in clusters 2 and 3, while the accessions in cluster 2 showed higher plasticity in the ERD and FRD than those in clusters 1 and 3 (Figure 2(b), Table S3). These findings demonstrated that accessions differed with respect to the plasticities of the four investigated focal traits. Next, using the CVs of the 77 accessions, we tested if the plasticities of the four focal traits correlated. We found that the CV of the ERD showed significant positive Spearman correlation with the CV of the FRD (0.42, *p*-value = 4.7×10^5) and FT (0.37, *p*-value = 5.7×10^{-5}), indicating that plasticity of the size in the beginning of vegetative growth is moderately associated with plasticity in flowering time (Figure 2(c)).

To investigate if the plasticity in the flowering time was due to change in the leaf initiation rate, we scored the number of rosette leaves until bolting for six accessions with varying plasticities of FT. We noted that under the same N condition, the total number

of leaves differed between the selected accessions, but all of them produced approximately twice the number of leaves under optimal N in comparison to the limiting N (Figure S1). This suggests that the earlier flowering under optimal N was due to a faster developmental transition to the reproductive phase.

3.2 | Genetic basis of plasticity of the growth- and flowering-related focal traits to N availability

Next, using genome-wide association (GWA) analysis, we investigated the genetic architecture of plasticity of the four studied focal traits in response to N. To this end, we performed the GWA using the CV over all three N conditions by using genotyping data with 250,000 SNPs (Horton et al., 2012). GWA analysis for the CVs of the four phenotypes identified only one significant biallelic association for FT at the end of chromosome 1 (*p*-value = 1.41×10^{-7}; Table 1 and Table S4, Methods). The lack of associations, when using CV as a measure for plasticity, could be due to large degree of noise in the data masking the detection of GWAs. The intermediate N condition was the most variable due to stochastic factors. For this reason, we performed the GWA with the fold changes (FC) of the phenotypic means between the optimal and limiting N conditions with the 250,000 SNPs. Interestingly, the GWA with the FC identified four SNPs on the same locus on chromosome 1 that was associated with the CV of FT (Table 1 and Table S4). We found no significant association for the other traits.

The low power of our dataset in detecting significant associations could be due to the low heritability (i.e., low proportion of genotype × environment variance from the total phenotypic variance) of the scored plasticities (Sasaki et al., 2015; Tam et al., 2019). To investigate the proportion of contribution of genetic (G), environmental (E) and genotype × environment (G × E) factors, we used mixed effect ANOVA. Since the accessions were grown in up to six batches, the variance components of the mixed-effect models were determined per batch (see Methods) for each of the complex traits. For ERD, the largest proportion of the variance, among the three factors was due to the environment in all of the batches (Figure S2(a)). For FRD and FT, there are batches where the predominant effects are due to the genotype (typical for FT) or the environment effect (Figure S2(b), (c)). For these traits, the average genotype effect over the five batches is similar to the average genotype-by-environment interaction effect. However, we found that in three of the five FT batches the variance due to genotype-by-environment interaction is larger than that due to genotype, indicating that there is variability in the responses of this trait to the different N availability (Figure S2(c)). Interestingly, for YIE, we also found that in three of the five batches the variance due to genotype-by-environment interaction dominates the variances due to the other factors (Figure S2(d)).

Another explanation for the low number of associations detected by the GWA is that the number of accessions that we used for our study did not suffice to identify the loci with small effects. A third explanation for the missing associations could be the incomplete set of SNPs, since the initial GWA was performed with 250,000 SNPs
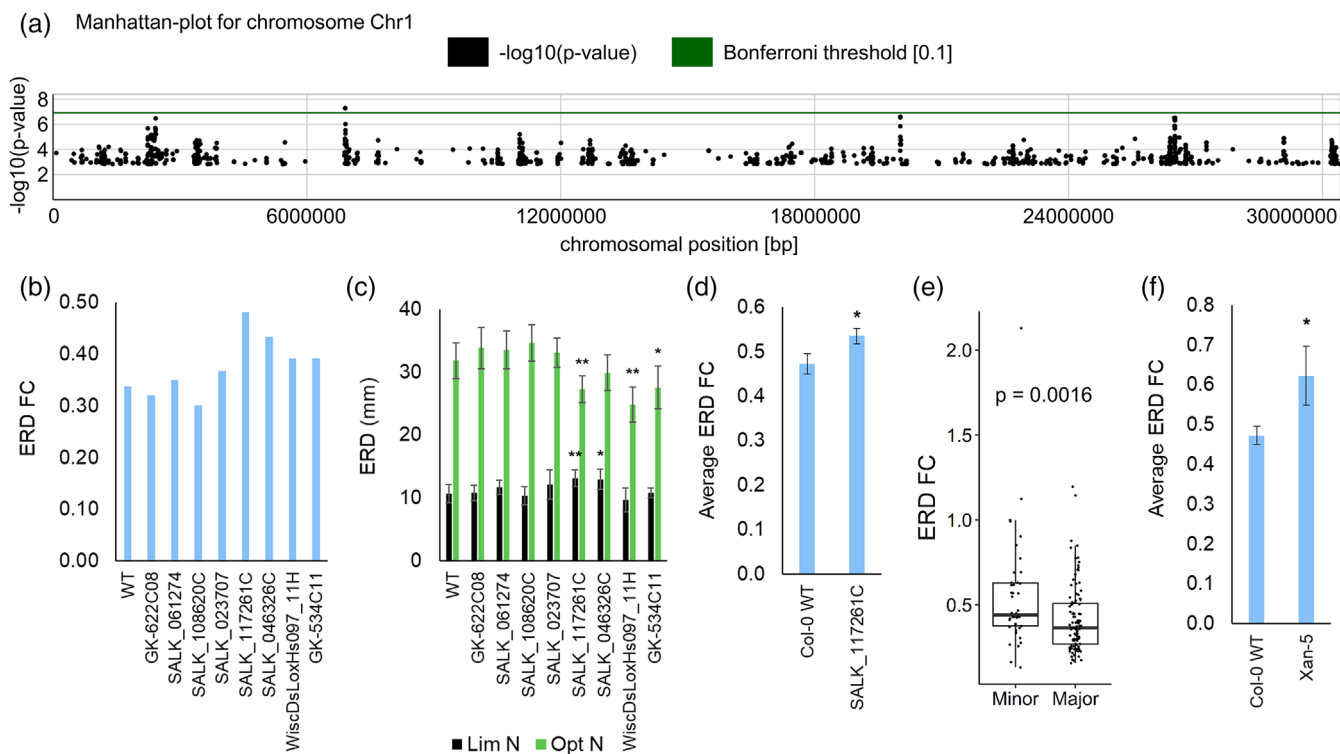
FIGURE 3 *Genetic architecture underlying plasticity of early rosette diameter (ERD) in response to N availability.* (a) Manhattan plot representing the significant association for fold change (FC) between optimal and limiting N of early rosette diameter (ERD) on chromosome 1. The analysis was run with easyGWAS (https://easygwas.ethz.ch/), using the sequenced genomes dataset ($n = 58$ accessions) with FaST-LMM and minimum allele frequency > 10%. The green line represents the Bonferroni significance level ($\alpha < 0.1$), and the associations are shown as dots ($-$log10 p-value). The chromosomal position (bp) is represented under the graph. (b) Fold change (FC) of early rosette diameter (ERD) for Col-0 WT and for the T-DNA lines of the candidate genes between the plants grown at limiting and at optimal N conditions ($n = 10$ replicates). (c) Early rosette diameter (ERD) of Col-0 WT and of the T-DNA lines grown under limiting (Lim) and optimal (Opt) N ($n = 10$ replicates). (d) Early rosette diameter (ERD) fold change (FC) between optimal and limiting N of SALK_177261 and Col-0 WT. The plots represent the average FC of four independent experiments ($n = 10$ replicates in each). (e) Boxplot representing the two haplogroups for the fold change (FC) between optimal and limited N of early rosette diameter (ERD), including the accessions which were sequenced in this work ($n = 148$ accessions). The significance of the difference between the haplogroups based on their early rosette diameter (ERD) FC was tested using Mann–Whitney U test. (f) Early rosette diameter (ERD) fold change (FC) between optimal and limiting N of Xan-5 and Col-0 WT. The plots represent the average FC of four independent experiments ($n = 10$ replicates in each). For panels (c), (d) and (f), significant differences to the Col-0 WT according to Mann–Whitney U test are represented by one (p-value < 0.05), or two (p-values < 0.01) asterisks above each column. The error bars indicate the standard deviation [Colour figure can be viewed at wileyonlinelibrary.com]

(Horton et al., 2012). To investigate if the lack of SNPs was the reason for the few detected associations, we took advantage of those accessions with fully sequenced genome, including 58 for ERD, 49 for FRD, 54 for FT and 44 for YIE, and performed GWA for the two plasticity scores. We detected a significant association for the ERD on chromosome 1–2 biallelic SNPs (Figure 3(a); Table 1 and Table S4).

Finally, we asked if the plasticity (scored as CV or FC) of the focal traits is controlled by the same genes that control the differences in the mean trait values in the accessions. To investigate this question, we performed the GWA with the mean value of the traits in the three N conditions. We found a single significant association for ERD at intermediate N on chromosome 1, but to a different SNP than that found for the plasticity of ERD (Methods, Table S1). This implies that the plasticity of the traits in response to N has a different genetic basis than the one controlling the mean trait value in a single condition.

3.3 | Characterization of the candidate gene using T-DNA lines

Based on the linkage disequilibrium, we considered genes that were located ±10 Kb and ± 20 Kb of the significantly associated SNPs for ERD and FT, respectively, as candidates. This resulted in eleven candidates around the SNPs associated with the plasticity of FT to N, and six candidate genes for the SNPs associated with the plasticity of ERD to N. To investigate the candidates, we examined 14 and 8 T-DNA mutant lines in Colombia (Col-0) background for the eleven and six candidate genes controlling the plasticity of FT and ERD, respectively (Table S4). After confirming the homozygosity of the T-DNA insertion, the lines were grown under the three N conditions as used for the initial screening, and the plasticity was compared to the Col-0 wild type (WT) in two independent experiments.

We did not detect significantly altered FC nor CV in FT in response to N in any of the tested mutant lines in comparison to Col-0 (Figure S3). We reasoned that the extremely low FT plasticity of Col-0 accession in response to N availability decreases the power for detecting significant differences. Indeed, the CV of FT ranged from 0.01 to 0.05 (Figure S3(d)) and the FC of FT ranged from 0.93 to 1.07 (Figure S3(e)), reflecting the low plasticity of this trait. For the ERD plasticity, homozygous T-DNA mutant lines for five of the candidate genes were identified and further characterized. The homozygous SALK_117261 line, with T-DNA insertion in *At1g19880* gene, exhibited approximately 80% reduced FC in ERD as compared to Col-0 in two independent experiments (Figure 3(b)). The reduced FC in ERD in the SALK_117261 line was due to significantly larger ERD under the limiting N condition and significantly reduced ERD at the optimal N (Figure 3(c)). For further statistical validation, we repeated the experiment four times and showed that the FC difference in ERD in response to N between SALK_117261 line and Col-0 WT was statistically significant (Figure 3(d)).

Analysis of homology demonstrated that *At1g19880* encodes for an uncharacterized regulator of chromosome condensation (RCC1) family protein, which we further named as *PLASTICITY OF ROSETTE SIZE TO NITROGEN 1* (*PROTON1*). The RCC1 family proteins include one or more RCC1- like domains (RLDs), and are known to have diverse function (Hadjebi et al., 2008). In Arabidopsis, there are 24 RCC1 family proteins, from which so far only UV RESISTANCE LOCUS 8 (UVR8) (Christie et al., 2012; Wu et al., 2012), RCC1/UVR8/GEF3-like 3 (RUG3) (Kuhn et al., 2011), TOLERANT TO CHILLING AND FREEZING 1 (TCF1) (Ji et al., 2015) and SENSITIVE TO ABA 1 (SAB1) (Ji et al., 2019) have been characterized.

3.4 | The role of *PROTON1* in controlling the plasticity of ERD in response to nitrogen

The significant association for plasticity of ERD in response to N availability was detected based on the SNPs of 58 fully sequenced accessions, but was not found when using the 250,000 SNPs due to the absence of the identified SNPs in this dataset. To provide additional support for this association, we sequenced the missing region in the 250,000 SNP data that contains the biallelic SNP for the 90 accessions that were included in the initial phenotyping panel (Table S5). We then looked at the associations of the sequenced SNP to the plasticity in ERD in response to N. From all analysed accessions, 42 carried the minor alleles (A and T, for positions 6,904,858 and 6,904,935, respectively) and 106 accessions carried the major alleles (C and G, respectively). On average, the accessions with minor alleles showed 25% lower FC in ERD in comparison to the accessions with major alleles (0.55 and 0.41, respectively) (Figure 3(e)). The difference between the ERD FC of the two haplogroups was significant ($p = 0.0016$, Mann Whitney *U* test), giving further support to the association of *PROTON1* to the ERD plasticity in response to N. To further confirm the role of *PROTON1* in controlling the plasticity of ERD to N availability, we searched the published genome sequences

of Arabidopsis accessions for polymorphisms in *PROTON1* (*At1g19880*) gene. We identified that Xan-5 has a missense substitution that results in the disruption of the start codon of *PROTON1*. The presence of this SNP in Xan-5 was further confirmed by sequencing. When we grew Xan-5 and Col-0 WT under optimal and limiting N (Figure S4), we observed reduction in the plasticity of ERD in Xan-5 as well, thus further supporting the proposed role of *PROTON1* in ERD plasticity in response to N (Figure 3(f)).

Gene expression analysis of rosette leaves of plants grown under limiting and optimal N revealed that *PROTON1* is a strong knockdown mutant, showing more than 1,000 times reduced expression of *PROTON1* in comparison to WT (Figure 4(a)). Furthermore, the expression of *PROTON1* was increased in WT under limiting N (Figure 4(b)). In addition, we observed that the *PROTON1* flowered slightly earlier than the WT under limiting N, but that its FT was not different from that of the WT under optimal N (Figure 4(c), (d)). To investigate if *PROTON1* controlled plasticity of ERD in response to N availability is due to the plasticity of N uptake, transport or assimilation; we evaluated the expression of 18 genes involved in these processes in WT and *PROTON1* mutant grown under either limiting or optimal N. From the 18 analysed genes, seven showed a significant expression difference between WT and the mutant line in both optimal and limiting conditions including the ammonium transporters *AMT1;1*, *AMT1;4*, *AMT2;1*; *NIA2*, involved in N assimilation; *NLP7* transcription factor; and *NRT1;5* and *NRT3;1*, which are nitrate transporters (Figure 4(e), (f)). Furthermore, the levels of N assimilation *NIA1* gene and *NLP1* transcription factor under limiting N, and the ammonium transporter *AMT1;2* and *NLP6* transcription factor were also significantly different between *PROTON1* and the WT under optimal N (Figure 4(f)). All of the transcripts that showed significantly perturbed expression had higher expression in the mutant line in comparison to the WT, indicating that *PROTON1* is involved in processes that lead to repression of expression of genes involved in the aforementioned N-related processes. In addition, it also suggests that the increased plasticity is associated with the increased expression of genes involved in N responses. The mechanism by which *PROTON1* modulates the expression of these genes remains unknown.

Finally, to test if *PROTON1* phenotype was a consequence of a general growth impairment rather than response to N, we compared the performance of *PROTON1* and Col-0 WT plants treated with 100 mM and 150 mM NaCl (Figure 4(g)). We observed no difference between *PROTON1* and the WT in response to salt stress (Figure 4(g)), thus supporting that *PROTON1* responses were not because of an altered growth rate as a result of an unspecific stress response.

3.5 | Metabolic changes associated with plasticity of studied phenotypes to N availability

Primary metabolism is associated with growth and levels of several primary metabolites are altered in response to changes in N availability (Sulpice et al., 2013). However, it is not clear if the plasticity of metabolites is associated with plasticity of the complex phenotypes
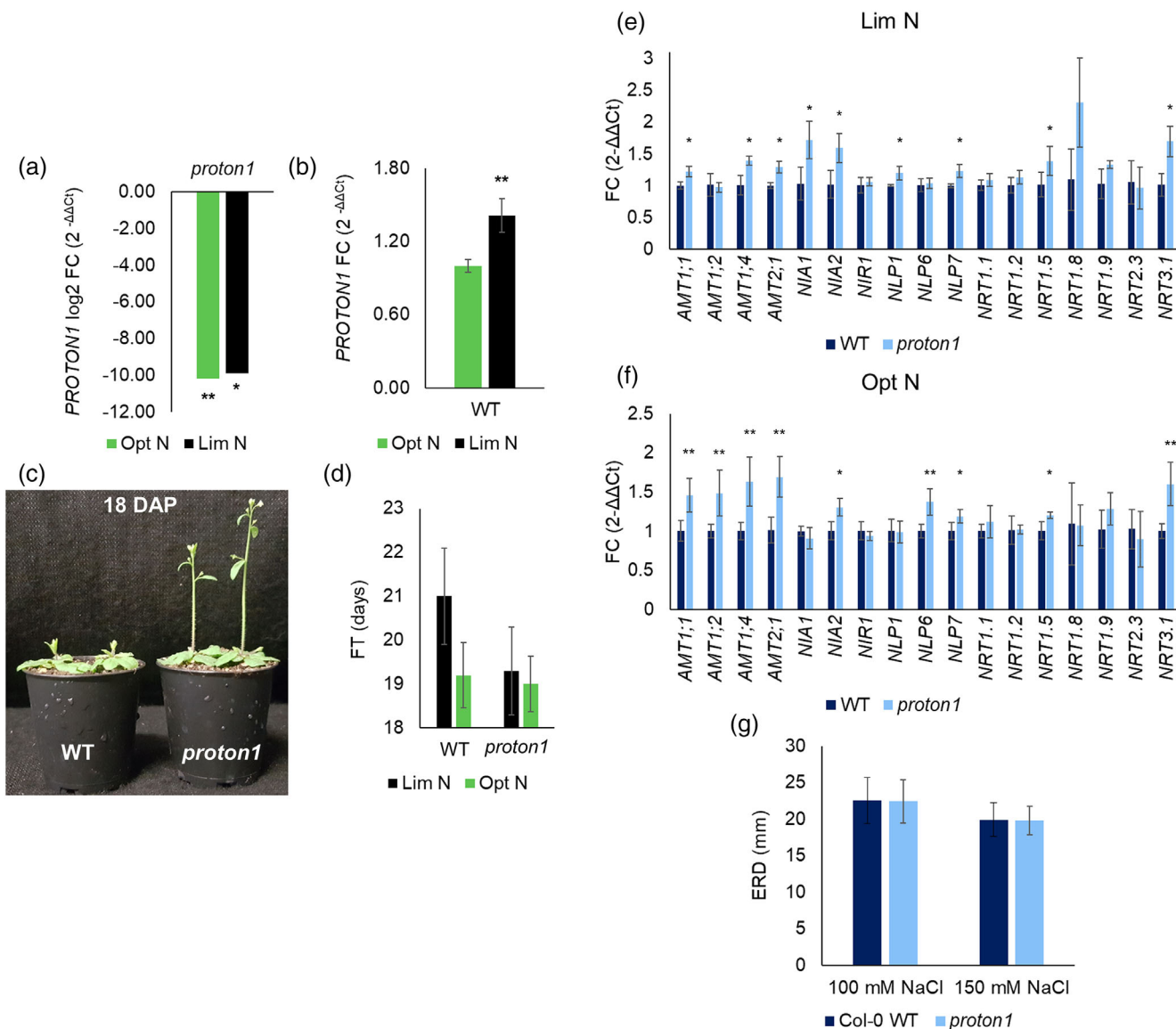
FIGURE 4 *The role of PROTON1 in plasticity of early rosette diameter (ERD) in response to N availability.* (a) Relative expression of *PROTON1* (*At1g19880*) in *PROTON1* T-DNA line, represented as the Log2 fold change (FC) in comparison to the Col-0 WT in each N conditions. (b) Relative expression of *PROTON1* (*At1g19880*) in Col-0 WT in response to limiting N (Lim), using the expression levels at optimal N (Opt) as reference. (c) Col-0 WT and *PROTON1* grown under limiting N. Photo was taken 18 days after pricking (DAP). (d) Number of days to the first open flower (FT) in Col-0 WT and *PROTON1* under both limiting and optimal N. (e) Relative expression of N-related genes in Col WT and *PROTON1* under limiting N, represented as the fold change (FC) to the WT (*n* = 5 replicates). (f) Relative expression of N-related genes in Col WT and *PROTON1* under optimal N, represented as the fold change (FC) to the WT (*n* = 5 replicates). (g) Early rosette diameter (ERD) of Col-0 WT and *PROTON1* T-DNA line grown under 100 mM NaCl and 150 mM NaCl stress (four independent experiments, *n* = 10 replicates in each). For all plots, significant differences to the WT according to Mann–Whitney U test are represented by one (*p*-value < 0.05), or two (*p*-value > 0.01) asterisks above each column. The error bars indicate the standard deviation [Colour figure can be viewed at wileyonlinelibrary.com]

studied here. To address this question, we first measured the levels of 66 primary metabolites in a subset of 43 accessions grown in the three N conditions (Table S6). To quantify plasticity, we calculated the CV of every metabolite across the three mean values for each of the 43 accessions (Table S7). The majority of primary metabolites are essential for plant growth and showed low plasticity across N conditions as expected (Figure 5(a)). The organic acids citrate and fumarate, and the amino acids ornithine, glutamine, lysine and arginine showed

the highest median CV across the accessions (Figure 5(a); Table S7). Of these, glutamine and glutamate are directly linked to N assimilation, whilst citrate is a precursor for 2-oxoglutarate needed in this process. Furthermore, malate and citrate valves are directly linked to carbon fixation and the tricarboxylic acid (TCA) cycle, providing the substrates for amino acids synthesis and their conversion can favour the accumulation of other metabolites, such as fumarate (Eprintsev et al., 2016).
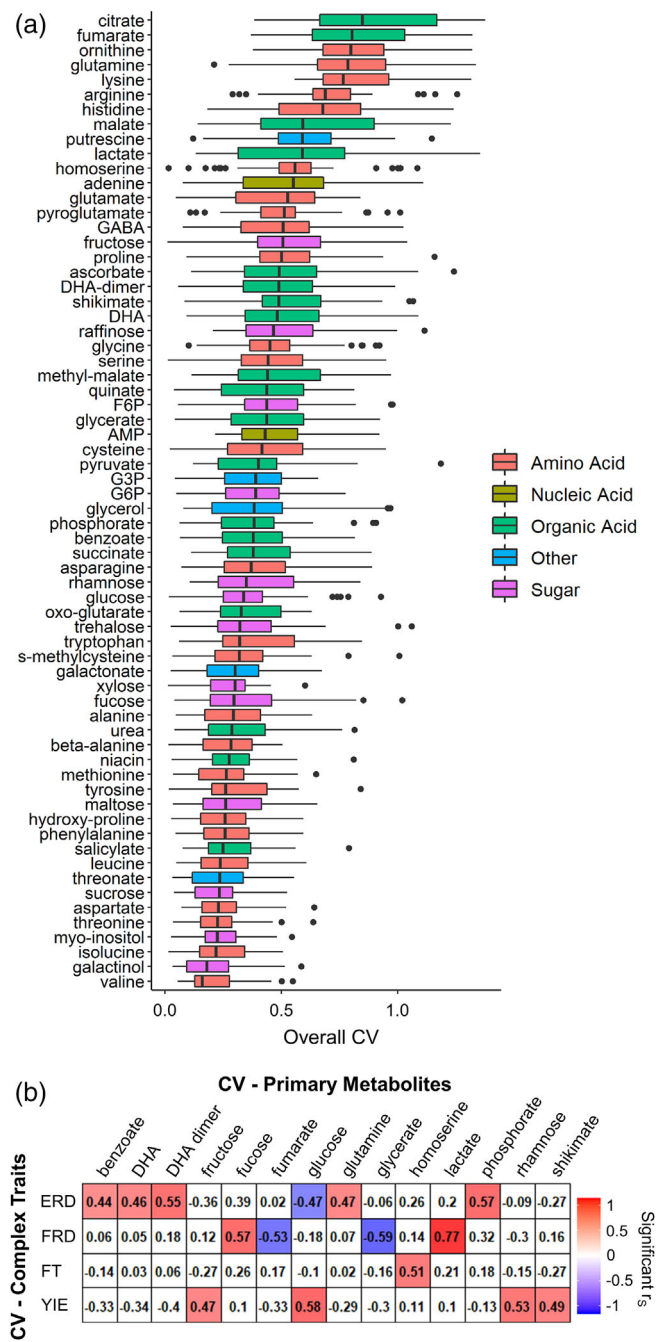
FIGURE 5 *Plasticity of primary metabolites in response to N availability of Arabidopsis accessions.* (a) Boxplots for coefficient of variation (CV) of each metabolite across accessions (*n* = 43 accessions, with at least three replicates each) grown under limiting, intermediate and optimal N. The metabolites are coloured according to their classification. (b) Metabolites which coefficient of variation (CV) levels showed significant correlation with plasticity of the four complex traits. Significant Spearman correlation after Benjamini-Hochberg correction (FDR < 0.05) are indicated as red for positive, or blue for negative. Abbreviations: adenosine-5-monophosphate (AMP), dehydroascorbate (DHA), fructose-6-phosphate (F6P), gamma aminobutyric acid (GABA), glucose-6-phosphate (G6P), glycerol-3-phosphate (G3P) [Colour figure can be viewed at wileyonlinelibrary.com]

To evaluate if metabolic plasticity relates to plasticity of the four phenotypes, we performed correlation analysis between the CVs of metabolites and CVs of phenotypes ERD, FRD, FT and YIE over the 43 accessions (Figure 5(b)). We found a significant positive correlation between the plasticity of ERD and plasticities of benzoate, dehydroascorbate (dimer), glutamine and phosphorate levels, and a significant negative correlation with plasticity of glucose levels. Therefore, our findings suggest that stable levels of glucose over different N conditions, in contrast to dehydroascorbate, are associated with the higher plasticity of ERD. Further, plasticity of FRD showed significant negative correlation with plasticity of fumarate and glycerate levels, and positive correlation with plasticities in lactate and fucose levels (Figure 5(b)). The plasticity of FT showed positive correlation with homoserine levels, while that of YIE positively correlated with plasticity of fructose, glucose, rhamnose and shikimate levels (Figure 5(b)). The latter indicates that stable sugar contents stabilizes yield in respond to N availability.

Next, we asked if a significant correlation was observed between the plasticity (CV) of a complex trait or metabolite level and the mean ERD, FRD, FT and YIE or metabolite level in each N condition separately (Figure S5). The heatmaps demonstrate that there are substantially less significant correlations between the means than between the means and CVs or between the CVs of the studied traits. This analysis supports the hypothesis that the plasticities and the mean values of the studied traits are independently regulated of the plasticity.

The largest number of significant correlations were unidentified under limiting N, followed by intermediate and optimal N availability. YIE exhibited significant correlations with the CVs of metabolite levels only under limiting N, while the mean of ERD, in the separate N conditions, appeared to exhibit the smallest number of significant correlations to the CVs of metabolite levels (Figure S5). Under limiting N, the mean of FRD was negatively correlated to the CV of fucose, G3P, lactate, phosphorate and quinate levels and positively correlated to the CV of glycerate levels (over all conditions) (Figure S5). The mean of FT was negatively correlated to the CV of benzoate, galactinol, glutamine, maltose and trehalose and the mean of YIE was negatively correlated to the CV of beta-alanine, fructose, glucose, G6P, G3P and serine levels and was positively correlated to the CV of DHA dimer and maltose (Figure S5). Interestingly, the CV of ERD was positively correlated to the mean of YIE in two of the three conditions (Figure S5).

3.6 | Accessions showed different degrees of ERD and FT plasticity in response to different environments

Our results showed that plasticity of different phenotypes to N availability are not under the control of the same loci, and that plasticity of specific phenotypes varied between the studied accessions. Next, we asked whether plasticities of ERD and FT are specific to certain environmental cues, or whether different accessions show similar
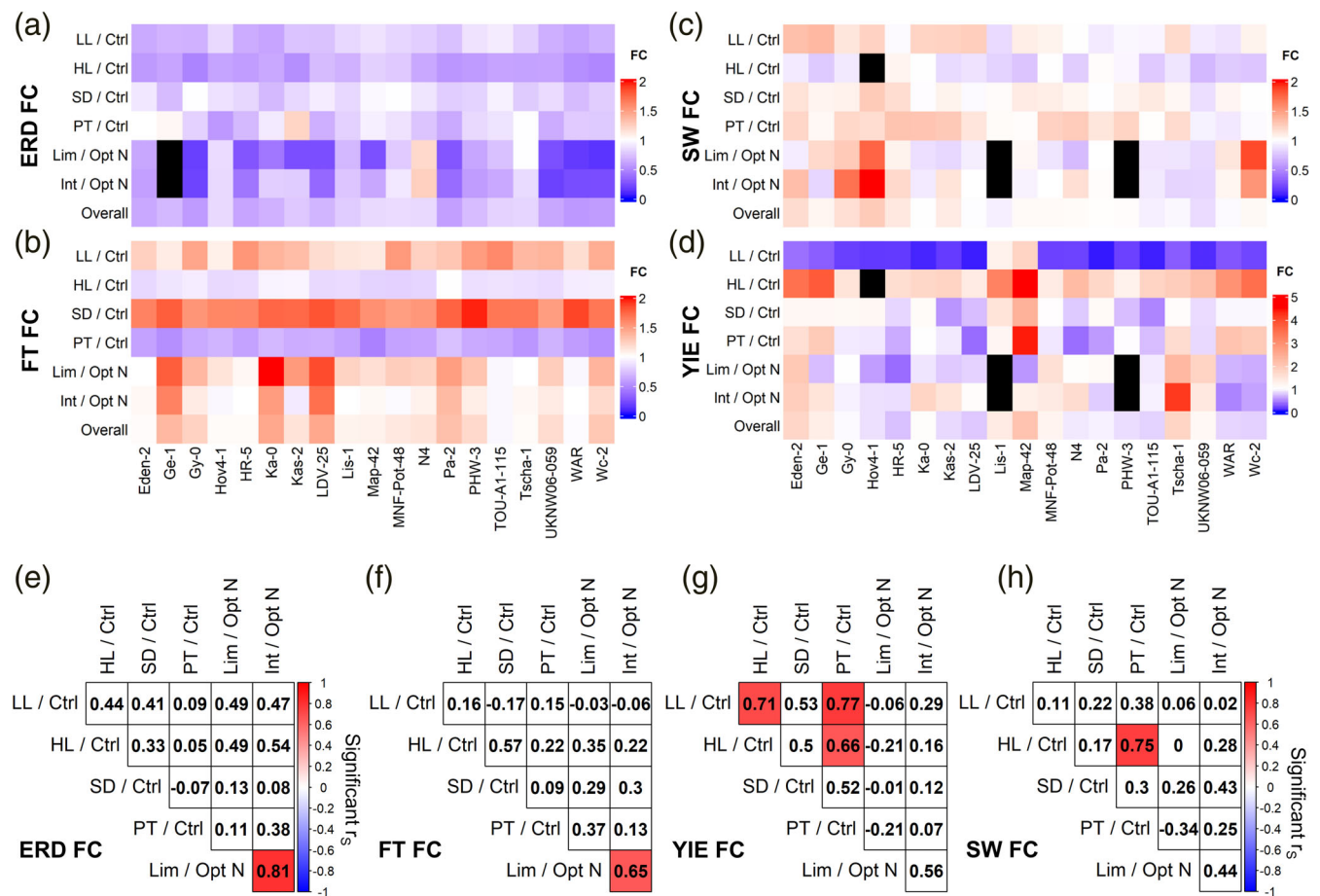
FIGURE 6 FI *Plasticity of early rosette diameter (ERD) and flowering time (FT) in response to different environments in Arabidopsis accessions.* Heatmaps representing the fold changes of 19 accessions (Table S8) for (a) early rosette diameter (ERD), (b) flowering time (FT), (c) yield (YIE) and (d) seed weight (SW) between the indicated conditions. The fold changes (FCs) were calculated for plants grown under low light (LL, $n = 10$ plants for each accession), high light (HL, $n = 15$ plants for each accession), short days (SD, $n = 10$ plants for each accession), or in the polytunnel (PT, $n = 15$ plants for each accession) in comparison to those grown under long days and normal lights (Ctrl, $n = 10$ plants for each accession). For the N responses, the FC was calculated based on the means of plants grown under limiting (Lim) or intermediate (Int) N to those grown under optimal (Opt) N during the N screening ($n = 4$ plants for each accession). The FC values are indicated on a scale ranging from 2 or 5 (red) to 0 (blue) in comparison to the control. Black denotes missing data. Pearson correlation analysis between the FCs of (e) early rosette diameter (ERD), (f) flowering time (FT), (g) yield (YIE) and (h) seed weight (SW) in the indicated conditions. Adjusted *p*-values were calculated using Benjamini-Hochberg correction. Significant Spearman r_s correlations (FDR < 0.05) are represented as red for positive, or blue for negative [Colour figure can be viewed at wileyonlinelibrary.com]

plasticities in ERD and FT independent of the environmental changes. To investigate this question, we selected 19 accessions, covering the range from low to high CVs for ERD, FT and YIE (Table S3). These accessions were grown at 20°C/16°C (day/night) in four additional environments known to impact plant growth, including long days (16 hr/8 hr) with low light (20 µE) and high light (750 µE), short day (8 hr/16 hr, 120 µE) and in the polytunnel with natural light and temperature conditions. Plants grown at 20°C/16°C (day/night) under long days with light intensity of 120 µE were used as control. In the polytunnel, the average temperature during the experiment was 26.2°C, with minimum of 11.5°C and a maximum of 59.5°C. Each accession was scored for ERD, FT and YIE. In addition to the total number of seeds (YIE), the average seed weight (SW) for each accession in each condition was also

estimated. To quantify the plasticity of ERD, FT, YIE and SW in response to the different conditions, we calculated the FC between each condition to the control condition (Figure 6(a)–(d); Table S8). To investigate whether the same accessions showed high plasticity in the phenotypes in response to all growth-limiting conditions, we conducted a correlation analysis of the plasticities of each trait in response to the different conditions for each accession (Figure 6(e)–(h)). We did not find any significant correlations between the FCs in response to N and light environments. Significant correlations were found for plasticities of ERD and FT in response to N, and for plasticities of YIE and SW in response to light. These results suggest that plasticities of ERD, FT, YIE and SW in response to different environmental cues (i.e., N and light) may have distinct underlying mechanisms.

4 | DISCUSSION

Plants cope with changing environments by adjusting their phenotype through phenotypic plasticity. The four adaptive phenotypes studied here, namely early and final rosette size, flowering time and seed yield, are known to respond to varying N availability (de Jong et al., 2019; Ikram et al., 2012; Masclaux-Daubresse & Chardon, 2011; Meyer et al., 2019; North et al., 2009). However, the genetic basis of their phenotypic plasticity in response to N availability is unknown. In this study, we quantified plasticity of the four phenotypes in response to N by using both CV and FC and used GWA analysis to identify candidate genes. None of the significantly associated loci contained genes known to be involved in N response. This suggests, supporting the finding by Kusmec et al. (2018), that the genetic basis of plasticity in response to N is independent from the mean value of the focal N-related traits. This was further supported with our observation that the loci associated to the mean trait value of the accessions in different N condition were different from the loci associated with the trait plasticities to N. By using T-DNA mutant lines for the candidate genes, we verified that a regulator of chromosome condensation (RCC1) family protein, named here as *PROTON1*, influenced the plasticity of ERD in response to N availability. The T-DNA mutant line for *PROTON1* (SALK_117261) showed significantly larger size under limiting N and was significantly smaller under optimal N (Figure 3(c)), resulting in reduced plasticity of ERD across the conditions (Figure 3(d)). This suggests that RCC1-mediated stability in growth is attained by improved performance in the limiting conditions, but with reduced performance in optimal conditions. Therefore, our findings point that *PROTON1* may mediate the trade-off between stable and maximal growth under different N conditions.

RCC1-family proteins were first identified to function in regulating cell cycle, but since then different members of this family are known to be involved in diverse functions (Hadjebi et al., 2008). Arabidopsis contains 24 RCC1-family genes, but only four of them have been characterized so far. *PROTON1* is the most highly expressed in roots and young leaves (BAR eFP Browser, Arabidopsis.org), and we found that it was induced by limiting N in young leaves (Figure 4(b)). Co-expression analysis of *PROTON1* showed that it is co-expressed with eight genes with function in the spliceosome machinery (Figure S6) that mediates alternative splicing plants. The four genes in primary co-expression network of *PROTON1* include two RNA-binding family protein members. One of these is SR34, a known splicing factors in Arabidopsis (Stankovic et al., 2016). The role of alternative splicing controlling *PROTON1*-mediated plasticity of ERD and FT in response to N availability remains to be investigated. Alternative splicing regulates gene expression and protein diversity by producing multiple mRNA isoforms from a single gene. In *Arabidopsis*, alternative splicing is known to regulate transitioning to flowering, but less is known how the alternative splicing is regulated by environmental cues. An intriguing question for future studies would be to investigate if variability in spliceosome, similar to the HSP90 system (Queitsch et al., 2002; Salathia & Queitsch, 2007; Sangster et al., 2008; Sangster & Queitsch, 2005; Zabinsky et al., 2019), plays a central role in regulating plasticity in plants and animals.

In addition to the genetic basis of plasticity, we used correlation analysis to investigate whether plasticity of specific primary metabolites was associated with the plasticity of any of the four phenotypes. We identified that plasticities of the fumarate and glycerate levels showed significant negative correlation with the plasticity of FRD. The mean levels of fumarate and glycerate were previously found to negatively correlate with the biomass of Arabidopsis plants grown under low N conditions (Sulpice et al., 2013). In our experiments, the mean levels of fumarate showed negative correlation with the mean ERD only under optimal N conditions (Figure S5(c)). This suggests, similar to the four phenotypes, that the mean metabolites levels associated with N responses are different from the plasticity of metabolite levels in response to N.

To rapidly respond to changes in surroundings, plasticity in an important trait for survival of homozygous organisms, such as Arabidopsis. We found that plasticities of ERD and FT and the plasticity of FRD correlated in across the studied accessions (Figure 2(c)). In addition, *PROTON1* mutant line was associated with both altered ERD and FT plasticity in response to N availability. Further, in *PROTON1*, the ERD and FT plasticities were due to a slightly faster development and earlier FT in limiting N conditions (Figure 4(c), (d)). These findings indicate that these traits respond simultaneously to the changing N. Furthermore, we found that the different environments had different impact on the focal traits. This enhances our understanding of the complexity of possible constraints and consequences of selection when acting on plasticity in response to climate change. Altogether, these results highlight the importance to investigate plasticity of different phenotypes in multiple environments alone and in combination, when understanding the past, present and future relationships between the plants and environment.

CONFLICT OF INTERESTS

The authors declare no conflict of interest.

AUTHOR CONTRIBUTIONS

G.T.D. did all data analysis, ran GWAS, identified and characterized T-DNA lines for the candidate genes, planned and performed the adaptability experiment, planned and conducted the qRT-PCR. All figures were made by G.T.D. P.P. conducted the initial screening and quantifications and extraction of metabolites. N.V. measured the early

rosette diameter and helped P.P. with the screening. S.A. measured metabolite levels. A.R.F. supervised metabolomics measurements. R.A.E.L. and Z.N. planned the experiments, R.A.E.L. supervised the experiments and Z.N. supervised the data analysis. R.A.E.L., G.T.D. and Z.N. wrote the manuscript. All authors have read the final version of the manuscript.

DATA AVAILABILITY STATEMENT

The data that supports the findings of this study are available in the supplementary material of this article.

ORCID

Gustavo Turqueto Duarte https://orcid.org/0000-0002-3248-4957
Roosa A. E. Laitinen https://orcid.org/0000-0003-3317-4667

REFERENCES

Alseekh, S., Tong, H., Scossa, F., Brotman, Y., Vigroux, F., Tohge, T., … Fernie, A. R. (2017). Canalization of tomato fruit metabolism. *Plant Cell*, *29*(11), 2753–2765. https://doi.org/10.1105/tpc.17.00367

Arsova, B., Kierszniowska, S., & Schulze, W. X. (2012). The use of heavy nitrogen in quantitative proteomics experiments in plants. *Trends in Plant Science*, *17*(2), 102–112. https://doi.org/10.1016/j.tplants.2011.11.001

Berendzen, K., Searle, I., Ravenscroft, D., Koncz, C., Batschauer, A., Coupland, G., … Ulker, B. (2005). A rapid and versatile combined DNA/RNA extraction protocol and its application to the analysis of a novel DNA marker set polymorphic between *Arabidopsis thaliana* ecotypes Col-0 and Landsberg erecta. *Plant Methods*, *1*, 4. https://doi.org/10.1186/1746-4811-1-4

Brachi, B., Faure, N., Bergelson, J., Cuguen, J., & Roux, F. (2013). Genome-wide association mapping of flowering time in *Arabidopsis thaliana* in nature: Genetics for underlying components and reaction norms across two successive years. *Acta Botanica Gallica*, *160*(3–4), 205–219. https://doi.org/10.1080/12538078.2013.807302

Christie, J. M., Arvai, A. S., Baxter, K. J., Heilmann, M., Pratt, A. J., O'Hara, A., … Getzoff, E. D. (2012). Plant UVR8 photoreceptor senses UV-B by tryptophan-mediated disruption of cross-dimer salt bridges. *Science*, *335*(6075), 1492–1496. https://doi.org/10.1126/science.1218091

de Jong, M., Tavares, H., Pasam, R. K., Butler, R., Ward, S., George, G., … Leyser, O. (2019). Natural variation in Arabidopsis shoot branching plasticity in response to nitrate supply affects fitness. *PLoS Genetics*, *15*(9), e1008366. https://doi.org/10.1371/journal.pgen.1008366

Eprintsev, A. T., Fedorin, D. N., Sazonova, O. V., & Igamberdiev, A. U. (2016). Light inhibition of fumarase in Arabidopsis leaves is phytochrome A-dependent and mediated by calcium. *Plant Physiology and Biochemistry*, *102*, 161–166. https://doi.org/10.1016/j.plaphy.2016.02.028

Evans, J. R., & Clarke, V. C. (2018). The nitrogen cost of photosynthesis. *Journal of Experimental Botany*, *70*(1), 7–15. https://doi.org/10.1093/jxb/ery366

Fredes, I., Moreno, S., Diaz, F. P., & Gutierrez, R. A. (2019). Nitrate signaling and the control of Arabidopsis growth and development. *Current Opinion in Plant Biology*, *47*, 112–118. https://doi.org/10.1016/j.pbi.2018.10.004

Gaudinier, A., Rodriguez-Medina, J., Zhang, L., Olson, A., Liseron-Monfils, C., Bagman, A. M., … Brady, S. M. (2018). Transcriptional regulation of nitrogen-associated metabolism and growth. *Nature*, *563*(7730), 259–264. https://doi.org/10.1038/s41586-018-0656-3

Grimm, D. G., Roqueiro, D., Salome, P. A., Kleeberger, S., Greshake, B., Zhu, W. S., … Borgwardt, K. M. (2017). easyGWAS: A cloud-based platform for comparing the results of genome-wide association studies. *Plant Cell*, *29*(1), 5–19. https://doi.org/10.1105/tpc.16.00551

Gu, Z. G., Eils, R., & Schlesner, M. (2016). Complex heatmaps reveal patterns and correlations in multidimensional genomic data. *Bioinformatics*, *32*(18), 2847–2849. https://doi.org/10.1093/bioinformatics/btw313

Guignard, M. S., Leitch, A. R., Acquisti, C., Eizaguirre, C., Elser, J. J., Hessen, D. O., … Leitch, I. J. (2017). Impacts of nitrogen and phosphorus: From genomes to natural ecosystems and agriculture. *Frontiers in Ecology and Evolution*, *5*(70), 1–9. https://doi.org/10.3389/fevo.2017.00070

Gutierrez, R. (2012). Nitrogen regulatory networks controlling plant root growth. *FEBS Journal*, *279*, 35–35.

Hadjebi, O., Casas-Terradellas, E., Garcia-Gonzalo, F. R., & Rosa, J. L. (2008). The RCC1 superfamily: From genes, to function, to disease. *Biochimica et Biophysica Acta*, *1783*(8), 1467–1479. https://doi.org/10.1016/j.bbamcr.2008.03.015

Horton, M. W., Hancock, A. M., Huang, Y. S., Toomajian, C., Atwell, S., Auton, A., … Bergelson, J. (2012). Genome-wide patterns of genetic variation in worldwide *Arabidopsis thaliana* accessions from the RegMap panel. *Nature Genetics*, *44*(2), 212–216. https://doi.org/10.1038/ng.1042

Ikram, S., Bedu, M., Daniel-Vedele, F., Chaillou, S., & Chardon, F. (2012). Natural variation of Arabidopsis response to nitrogen availability. *Journal of Experimental Botany*, *63*(1), 91–105. https://doi.org/10.1093/jxb/err244

Ji, H., Wang, S., Cheng, C., Li, R., Wang, Z., Jenkins, G. I., … Li, X. (2019). The RCC1 family protein SAB1 negatively regulates ABI5 through multidimensional mechanisms during postgermination in Arabidopsis. *New Phytologist*, *222*(2), 907–922. https://doi.org/10.1111/nph.15653

Ji, H., Wang, Y., Cloix, C., Li, K., Jenkins, G. I., Wang, S., … Li, X. (2015). The Arabidopsis RCC1 family protein TCF1 regulates freezing tolerance and cold acclimation through modulating lignin biosynthesis. *PLoS Genetics*, *11*(9), e1005471. https://doi.org/10.1371/journal.pgen.1005471

Joseph, B., Corwin, J. A., & Kliebenstein, D. J. (2015). Genetic variation in the nuclear and organellar genomes modulates stochastic variation in the metabolome, growth, and defense. *PLoS Genetics*, *11*(1), e1004779. https://doi.org/10.1371/journal.pgen.1004779

Kassambara, A. A. M. F. (2020). Factoextra: Extract and visualize the results of multivariate data analyses. R package version 1.0.7. https://CRAN.R-project.org/package=factoextra.

Kramer, U. (2015). Planting molecular functions in an ecological context with *Arabidopsis thaliana*. *eLife*, *4*, e06100. https://doi.org/10.7554/eLife.06100

Krapp, A., Berthomé, R., Orsel, M., Mercey-Boutet, S., Yu, A., Castaings, L., … Daniel-Vedele, F. (2011). Arabidopsis roots and shoots show distinct temporal adaptation patterns toward nitrogen starvation. *Plant Physiology*, *157*(3), 1255–1282. https://doi.org/10.1104/pp.111.179838

Kuhlmann, M., Meyer, R. C., Jia, Z. T., Klose, D., Krieg, L. M., von Wiren, N., & Altmann, T. (2020). Epigenetic variation at a genomic locus affecting biomass accumulation under low nitrogen in *Arabidopsis thaliana*. *Agronomy-Basel*, *10*(5), 636. https://doi.org/10.3390/agronomy10050636

Kuhn, K., Carrie, C., Giraud, E., Wang, Y., Meyer, E. H., Narsai, R., … Whelan, J. (2011). The RCC1 family protein RUG3 is required for splicing of nad2 and complex I biogenesis in mitochondria of *Arabidopsis thaliana*. *Plant Journal*, *67*(6), 1067–1080. https://doi.org/10.1111/j.1365-313X.2011.04658.x

Kusmec, A., de Leon, N., & Schnable, P. S. (2018). Harnessing phenotypic plasticity to improve maize yields. *Frontiers in Plant Science*, *9*, 1377. https://doi.org/10.3389/fpls.2018.01377

Laitinen, R. A. E., & Nikoloski, Z. (2019). Genetic basis of plasticity in plants. *Journal of Experimental Botany*, *70*(3), 739–745. https://doi.org/10.1093/jxb/ery404

Lark, R. M., Milne, A. E., Addiscott, T. M., Goulding, K. W. T., Webster, C. P., & O'Flaherty, S. (2004). Scale- and location-dependent correlation of nitrous oxide emissions with soil properties: An analysis using wavelets. *European Journal of Soil Science*, 55(3), 611–627. https://doi.org/10.1111/j.1365-2389.2004.00620.x

Li, H., Hu, B., & Chu, C. C. (2017). Nitrogen use efficiency in crops: Lessons from Arabidopsis and rice. *Journal of Experimental Botany*, 68(10), 2477–2488. https://doi.org/10.1093/jxb/erx101

Lisec, J., Schauer, N., Kopka, J., Willmitzer, L., & Fernie, A. R. (2006). Gas chromatography mass spectrometry-based metabolite profiling in plants. *Nature Protocols*, 1(1), 387–396. https://doi.org/10.1038/nprot.2006.59

Masclaux-Daubresse, C., & Chardon, F. (2011). Exploring nitrogen remobilization for seed filling using natural variation in *Arabidopsis thaliana*. *Journal of Experimental Botany*, 62(6), 2131–2142. https://doi.org/10.1093/jxb/erq405

McAllister, C. H., Beatty, P. H., & Good, A. G. (2012). Engineering nitrogen use efficient crop plants: The current status. *Plant Biotechnology Journal*, 10(9), 1011–1025. https://doi.org/10.1111/j.1467-7652.2012.00700.x

Meyer, R. C., Gryczka, C., Neitsch, C., Muller, M., Brautigam, A., Schlereth, A., ... Altmann, T. (2019). Genetic diversity for nitrogen use efficiency in *Arabidopsis thaliana*. *Planta*, 250(1), 41–57. https://doi.org/10.1007/s00425-019-03140-3

North, K. A., Ehlting, B., Koprivova, A., Rennenberg, H., & Kopriva, S. (2009). Natural variation in Arabidopsis adaptation to growth at low nitrogen conditions. *Plant Physiology and Biochemistry*, 47(10), 912–918. https://doi.org/10.1016/j.plaphy.2009.06.009

Oldroyd, G. E. D., & Leyser, O. (2020). A plant's diet, surviving in a variable nutrient environment. *Science*, 368(6486), 45, eaba0196. https://doi.org/10.1126/science.aba0196

Pandey, P. K., Yu, J., Omranian, N., Alseekh, S., Vaid, N., Fernie, A. R., ... Laitinen, R. A. E. (2019). Plasticity in metabolism underpins local responses to nitrogen in *Arabidopsis thaliana* populations. *Plant Direct*, 3(11), e00186. https://doi.org/10.1002/pld3.186

Pennacchi, J. P., de Sousa Lira, J. M., Rodrigues, M., Garcia, F. H., Mendonca, A., & Delfino Barbosa, J. (2020). A systemic approach to the quantification of the phenotypic plasticity of plant physiological traits: The MVPi. *Journal of Experimental Botany*, 72, 1864–1878. https://doi.org/10.1093/jxb/eraa545

Perchlik, M., & Tegeder, M. (2017). Improving plant nitrogen use efficiency through alteration of amino acid transport processes. *Plant Physiology*, 175(1), 235–247. https://doi.org/10.1104/pp.17.00608

Queitsch, C., Sangster, T. A., & Lindquist, S. (2002). Hsp90 as a capacitor of phenotypic variation. *Nature*, 417(6889), 618–624. https://doi.org/10.1038/nature749

Revelle, W. (2020). Psych: Procedures for psychological, psychometric, and personality research. In *R package version 2.0.9*. Evanston, Illinois: Northwestern University.

Salathia, N., & Queitsch, C. (2007). Molecular mechanisms of canalization: Hsp90 and beyond. *Journal of Biosciences*, 32(3), 457–463. https://doi.org/10.1007/s12038-007-0045-9

Sangster, T. A., & Queitsch, C. (2005). The HSP90 chaperone complex, an emerging force in plant development and phenotypic plasticity. *Current Opinion in Plant Biology*, 8(1), 86–92. https://doi.org/10.1016/j.pbi.2004.11.012

Sangster, T. A., Salathia, N., Lee, H. N., Watanabe, E., Schellenberg, K., Morneau, K., ... Lindquist, S. (2008). HSP90-buffered genetic variation is common in *Arabidopsis thaliana*. *Proceedings of the National Academy of Sciences of the United States of America*, 105(8), 2969–2974. https://doi.org/10.1073/pnas.0712210105

Sasaki, E., Zhang, P., Atwell, S., Meng, D., & Nordborg, M. (2015). "missing" G x E variation controls flowering time in *Arabidopsis thaliana*. *PLoS Genetics*, 11(10), e1005597. https://doi.org/10.1371/journal.pgen.1005597

Scheible, W. R., Morcuende, R., Czechowski, T., Fritz, C., Osuna, D., Palacios-Rojas, N., ... Stitt, M. (2004). Genome-Wide reprogramming of primary and secondary metabolism, protein synthesis, cellular growth processes, and the regulatory infrastructure of arabidopsis in response to nitrogen. *Plant Physiology*, 136(1), 2483–2499. http://doi.org/10.1104/pp.104.047019

Schneider, C. A., Rasband, W. S., & Eliceiri, K. W. (2012). NIH image to ImageJ: 25 years of image analysis. *Nature Methods*, 9(7), 671–675. https://doi.org/10.1038/nmeth.2089

Stankovic, N., Schloesser, M., Joris, M., Sauvage, E., Hanikenne, M., & Motte, P. (2016). Dynamic distribution and interaction of the Arabidopsis SRSF1 subfamily splicing factors. *Plant Physiology*, 170(2), 1000–1013. https://doi.org/10.1104/pp.15.01338

Sulpice, R., Nikoloski, Z., Tschoep, H., Antonio, C., Kleessen, S., Larhlimi, A., ... Stitt, M. (2013). Impact of the carbon and nitrogen supply on relationships and connectivity between metabolism and biomass in a broad panel of Arabidopsis accessions. *Plant Physiology*, 162(1), 347–363. https://doi.org/10.1104/pp.112.210104

Tam, V., Patel, N., Turcotte, M., Bosse, Y., Pare, G., & Meyre, D. (2019). Benefits and limitations of genome-wide association studies. *Nature Reviews Genetics*, 20(8), 467–484. https://doi.org/10.1038/s41576-019-0127-1

Team, R. C. (2020). *A language and environment for statistical computing*. Vienna: Austria.

Vidal, E. A., & Gutierrez, R. A. (2008). A systems view of nitrogen nutrient and metabolite responses in Arabidopsis. *Current Opinion in Plant Biology*, 11(5), 521–529. https://doi.org/10.1016/j.pbi.2008.07.003

Wei, T. A. S. W. (2017). R package "corrplot": Visualization of a Correlation Matrix (version 0.84). https://github.com/taiyun/corrplot.

Weigel, D. (2012). Natural variation in Arabidopsis: From molecular genetics to ecological genomics. *Plant Physiology*, 158(1), 2–22. https://doi.org/10.1104/pp.111.189845

Wickham, H. (2009). *Ggplot2: Elegant Graphics for Data Analysis* (pp. 1–212). New York: Springer Science+Business Media. https://doi.org/10.1007/978-0-387-98141-3

Wickham, H. (2011). The split-apply-combine strategy for data analysis. *Journal of Statistical Software*, 40(1), 1–29. https://doi.org/10.18637/jss.v040.i01

Wickham, H. (2020). Tidyr: Tidy messy data. R package version 1.1.2. https://CRAN.R-project.org/package=tidyr.

Wu, D., Hu, Q., Yan, Z., Chen, W., Yan, C., Huang, X., ... Shi, Y. (2012). Structural basis of ultraviolet-B perception by UVR8. *Nature*, 484(7393), 214–219. https://doi.org/10.1038/nature10931

Zabinsky, R. A., Mason, G. A., Queitsch, C., & Jarosz, D. F. (2019). It's not magic-Hsp90 and its effects on genetic and epigenetic variation. *Seminars in Cell & Developmental Biology*, 88, 21–35. https://doi.org/10.1016/j.semcdb.2018.05.015

SUPPORTING INFORMATION

Additional supporting information may be found online in the Supporting Information section at the end of this article.